ASC Report No. 28/2014

A high order space momentum discontinuous Galerkin method for the Boltzmann equation

G. Kitzler and J. Schöberl

Institute for Analysis and Scientific Computing Vienna University of Technology — TU Wien
www.asc.tuwien.ac.at ISBN 978-3-902627-05-6

Most recent ASC Reports

27/2014 *W. Auzinger, T. Kassebacher, O. Koch, and M. Thalhammer*
Adaptive splitting methods for nonlinear Schrödinger equations in the semiclassical regime

26/2014 *W. Auzinger, R. Stolyarchuk, and M. Tutz*
Defect correction methods, classic and new (in Ukrainian)

25/2014 *J.M. Melenk and T.P. Wihler*
A posteriori error analysis of hp-FEM for singularly perturbed problems

24/2014 *J.M. Melenk and C. Xenophontos*
Robust exponential convergence of hp-FEM in balanced norms for singularly perturbed reaction-diffusion equations

23/2014 *M. Feischl, G. Gantner, and D. Praetorius*
Reliable and efficient a posteriori error estimation for adaptive IGA boundary element methods for weakly-singular integral equations

22/2014 *W. Auzinger, O. Koch, and M. Thalhammer*
Defect-based local error estimators for high-order splitting methods involving three linear operators

21/2014 *A. Jüngel and N. Zamponi*
Boundedness of weak solutions to cross-diffusion systems from population dynamics

20/2014 *A. Jüngel*
The boundedness-by-entropy principle for cross-diffusion systems

19/2014 *D. Boffi, L. Gastaldi, M. Ruggeri*
Mixed formulation for interface problems with distributed Lagrange multiplier

18/2014 *M. Halla, T. Hohage, L. Nannen. J. Schöberl*
Hardy Space Infinite Elements for Time-Harmonic Wave Equations with Phase Velocities of Different Signs

Institute for Analysis and Scientific Computing
Vienna University of Technology
Wiedner Hauptstraße 8–10
1040 Wien, Austria

E-Mail: admin@asc.tuwien.ac.at
WWW: http://www.asc.tuwien.ac.at
FAX: +43-1-58801-10196

ISBN 978-3-902627-05-6

ASC TU WIEN

A HIGH ORDER SPACE MOMENTUM DISCONTINUOUS GALERKIN METHOD FOR THE BOLTZMANN EQUATION

G. KITZLER* AND J. SCHÖBERL†

Abstract. In this paper we present a Discontinuous Galerkin method for the Boltzmann equation. The distribution function f is approximated by a shifted Maxwellian times a polynomial in space and momentum, while the test functions are chosen as polynomials. The first property leads to consistency with the Euler limit, while the second property ensures conservation of mass, momentum and energy. The focus of the paper is on efficient algorithms for the Boltzmann collision operator. We transform between nodal, hierarchical and polar polynomial bases to reduce the inner integral operator to diagonal form.

Key words. Boltzmann equation, Discontinuous Galerkin methods

1. Introduction. In this paper we present a numerical scheme for the Boltzmann equation. We will concentrate on the development of an efficient realization of the collision operator.

The numerical solution of the Boltzmann equation is a huge challenge, due to the high dimensionality (3 spatial + 3 momentum + 1 time variable) and the five fold integral defining the collision operator. Moreover, since the collision operator is closely connected to macroscopic conservation properties of the equation, it's integration has to be carried out with care.

Many authors focus on stochastic approaches such as Monte Carlo simulation. These were exploited by Bird [1] and Nanbu [2]. In [3] it was shown – for the space homogeneous situation – that the computational effort for both methods can be bounded by $\mathcal{O}(N)$, where N is the number of simulated particles. Typically these methods have to deal with stochastic fluctuation.

In deterministic approaches, the complexity of the high dimensional integration for the collision operator is a real challenge. Fourier transformation of the collision integral yields – for certain collision kernels – a significant simplification and moreover offers the possibility to use fast Fourier transform. For Maxwellian gases, the Fourier representation of the collision operator has a relatively simple form [4]. This specific representation was used in [5] to construct an efficient difference scheme. In [6] they extended their ideas to the case of hard sphere interaction. Another attempt using Fourier techniques was made in [7] were a Fourier series expansion of the solution function was combined with a finite difference scheme. A similar approach, based on truncated Fourier series approximation of the distribution function, but also on a Galerkin projection was presented in [8]. Typically these methods require a truncation of the momentum domain – for the solution function and also for the collision integrals – resulting in a perturbation of the conservation properties. In addition by adding periodicity to the solution function additional aliasing errors occur.

In this paper we present a Discontinuous Galerkin scheme in space and momentum. The global trial functions which represent the solution function in addition with Gauss-Hermite quadrature rules enables us to calculate the integrals over the unbounded velocity domain without truncating the integration domain. Moreover we

*Institute for Analysis and Scientific Computing, Vienna University of Technology, Austria. (gerhard.kitzler@tuwien.ac.at). Questions, comments, or corrections to this document may be directed to that email address.

†Institute for Analysis and Scientific Computing, Vienna University of Technology, Austria. (joachim.schoeberl@tuwien.ac.at)

do not need compact support for our solution function. Our trial space also consists of Maxwellian distributions, such that we are capable to represent the equilibrium solution of the space homogeneous problem exact. In section 2 we present the equation with its boundary conditions we want to solve. In section 3 we present the discretization in space, momentum and time. Section 4 deals with efficient application of the collision integrals. Therefore we do a basis transformation in the momentum domain to generalized Laguerre Polynomials giving us the possibility to perform the integration of the collision integrals efficiently. In the end, numerical results including space homogeneous and inhomogeneous examples shall demonstrate the possibilities of the method.
A close connection exists to the approach investigated in [9], were the solution is also expanded to generalized Laguerre polynomials with a Maxwellian weighting factor. In their work, they generalize the approach from [10] to radially non symmetric solutions.
For the transport operator, similar approaches are presented in [11, 12], where a Discontinuous Galerkin projection is applied to the Vlasslov-Poisson System. In contrast to our method, they use local polynomials in space and velocity direction.

2. The model. We consider a rarefied gas in a spatial domain $\Omega \subset \mathbb{R}^2$. The gas is described by a particle distribution function $f = f(t, x, v) \geq 0$. f has the usual meaning, such that $f(t_0, x_0, v_0)$ gives the average number of particles having position close to x_0 and velocity close to v_0 at time t_0. The time evolution of f is governed by the Boltzmann equation [13, 14, 15]:

$$\frac{\partial}{\partial t} f + \operatorname{div}_x(vf) = \frac{1}{k_n} Q(f) \qquad x \in \Omega, v \in \mathbb{R}^2, t \geq 0. \tag{2.1}$$

div_x is the divergence operator with respect to the spatial coordinate x. k_n is the knudsen number, representing the mean free path for the particles between subsequent collisions. $Q(f)$ is the Boltzmann collision operator given by:

$$Q(f)(t,x,v) := \int_{\mathbb{R}^2} \int_{S^1} B(v, w, e') \left[f(t,x,v') f(t,x,w') - f(t,x,v) f(t,x,w) \right] de\, dw. \tag{2.2}$$

The collision cross-section $B = B(v, w, e') = B(|v-w|, \frac{(v-w)\cdot e'}{|v-w|})$ is the probability for a binary collision of particles with pre collision velocities v and w and post collision velocities v' and w' to happen. We demand the collision cross-section to be separable such that $B(|v-w|, \frac{(v-w)\cdot e'}{|v-w|}) = b_r(|v-w|) b_\theta(\frac{(v-w)\cdot e'}{|v-w|})$. Moreover, the function b_θ has to satisfy Grad's cutoff assumption:

$$\int_0^{2\pi} b_\theta(s)\, ds < \infty.$$

In addition, the function b_r is demanded to have a power law dependency on its argument $|v-w|$, such that $b_r(r) = r^\beta$, for some exponent $\beta \in (-3, 1)$. These assumptions are natural for a wide range of collision kernels.

By conservation of mass, momentum and energy, the following, unique representation for the post collision velocities in terms of the scattering vector $e' \in S^1$ is found:

$$v' = \frac{v+w}{2} + e' \frac{|v-w|}{2} \qquad w' = \frac{v+w}{2} - e' \frac{|v-w|}{2} \qquad e' \in S^1. \tag{2.3}$$

In addition an initial condition $f(0,x,v) = f_0(x,v)$, describing the gas at time $t = 0$ and also boundary conditions describing the behaviour at $\partial\Omega$ have to be imposed. As a preparation we introduce the incoming and outgoing directions:

$$\mathbb{R}^2_{\text{in}} := \{v \in \mathbb{R}^2 : \langle v, n\rangle < 0\} \quad \text{and} \quad \mathbb{R}^2_{\text{out}} := \mathbb{R}^2 \setminus \mathbb{R}^2_{\text{in}},$$

where n is the outer normal vector in a point $x \in \partial\Omega$. Due to readability we suppress the x dependency of these sets.

Boundary conditions:

(i) specular reflection:

$$f(t,x,v) = f(t,x,v - 2\langle n(x), v\rangle n(x)) \quad \forall v \in \mathbb{R}^2_{\text{in}}. \tag{2.4a}$$

Particles hitting the wall behave like billiard balls. The tangential component of the particles' velocity does not change, while the normal component is multiplied by -1. Since $v - 2\langle v, n\rangle n \in \mathbb{R}^2_{\text{out}}$, this boundary condition states a direct relation between incoming and outgoing particles.

(ii) diffuse reflection:

$$f(t,x,v) = ce^{-\left|\frac{v-V_{\text{bnd}}}{\sqrt{T_{\text{bnd}}}}\right|^2} \int\limits_{\mathbb{R}^2_{\text{out}}} f(t,x,w)\langle w, n\rangle \, dw \quad \forall v \in \mathbb{R}^2_{\text{in}}, \tag{2.4b}$$

with $c > 0$ being a normalization constant for the flux of the Maxwellian distribution function (e.g. $c = \left(\int_{\mathbb{R}^2_{\text{in}}} e^{-\left|\frac{v-V_{\text{bnd}}}{\sqrt{T_{\text{bnd}}}}\right|^2} |\langle w, n(x)\rangle| \, dw \right)^{-1}$). The normalization guarantees that the total incoming and outgoing flux are the same:

$$\int_{\mathbb{R}^2_{\text{in}}} f(t,x,w)|\langle w, n(x)\rangle| \, dw = \int_{\mathbb{R}^2_{\text{out}}} f(t,x,w)|\langle w, n(x)\rangle| \, dw.$$

This is the only relation between in and outgoing values of f in this case. The behaviour of particles hitting the wall is affected by the temperature and velocity of the wall and also the total outgoing flux.

(iii) inflow boundary condition:

$$f(t,x,v) = f_{\text{in}}(t,x,v) \quad \forall v \in \mathbb{R}^2_{\text{in}}, \tag{2.4c}$$

with f_{in} being some given, non-negative distribution function at the boundary. In this case, there is no relation between incoming and outgoing values of f.

3. Discontinuous Galerkin Discretization. Our goal is to discretize (2.1) by a discontinuous Galerkin method. Therefore we multiply (2.1) with a test function $\phi = \phi(x,v)$ and integrate over the spatial and momentum domain:

$$\frac{\partial}{\partial t} \int\limits_{\Omega\times\mathbb{R}^2} f\phi \, d(x,v) + \int\limits_{\Omega\times\mathbb{R}^2} \operatorname{div}_x(vf)\phi \, d(x,v) = \int\limits_{\Omega\times\mathbb{R}^2} \frac{1}{k_n} Q(f)\phi \, d(x,v). \tag{3.1}$$

As usual we use discontinuous polynomial test and trial functions on a finite element mesh $\mathcal{T}_h$ in the spatial variable x. To obtain conservation of mass, momentum and energy we choose also polynomial test functions in momentum. The kernel of the

collision operator $Q(f(t,x,.))$ are the Maxwell distributions $M_{V,T}(v) := \frac{\rho}{2T\pi} e^{-\left|\frac{v-V}{\sqrt{T}}\right|^2}$. Since we aim in accurate approximation of solutions close to equilibrium, we choose trial functions as polynomials multiplied with a Maxwellian in momentum. To fix notation, we define the mesh $\mathcal{T}_h = \{K_1, \dots K_r\}$, h being the usual mesh size parameter and $V_N := P^N(\mathbb{R}^2)$. The trial space on one element $K \in \mathcal{T}_h$ is $V_K := P^k(K)$, and the global space on the domain Ω is denoted as $V_h^{\mathrm{DG}} := \prod_{K\in\mathcal{T}_h} V_K$. The space-momentum test space is denoted as

$$V_{h,N} = V_h^{\mathrm{DG}} \otimes V_N.$$

The trial space depends also on parameters $\overline{V}$ and $\overline{T}$, closely related to the macroscopic bulk velocity $V(x)$ and temperature $T(x)$. These parameters are assumed to be piecewise constants with notation $\overline{V}\big|_K \equiv \overline{V}_K$ and $\overline{T}\big|_K \equiv \overline{T}_K$. The resulting space is denoted as

$$\widetilde{V}_{h,N} = \prod_{K\in\mathcal{T}_h} V_K \otimes e^{-\left|\frac{v-\overline{V}_K}{\sqrt{\overline{T}_K}}\right|^2} V_N$$

The space $\widetilde{V}_{h,N}$ has dimension $\mathrm{ndof} := \sum_{K\in\mathcal{T}_h} \dim(V_K)\dim(V_N)$. The shorthand notation for element wise degrees of freedom is $\dim(V_K) =: \mathrm{ndof}_x$ and for the momentum space $\dim(V_N) =: \mathrm{ndof}_v$. The Maxwellian weight factor for the polynomials is denoted as element Maxwellian $M_{\overline{V}_K,\overline{T}_K}$.
The discontinuous Galerkin method is obtained by element-wise integration by parts of the transport term in (3.1). Assuming sufficient regularity, the exact solution f satisfies:

$$\frac{\partial}{\partial t} \sum_{K\in\mathcal{T}_h} \left(\int_{K\times\mathbb{R}^2} f\phi + \int_{\partial(K)\times\mathbb{R}^2} vf\phi n - \int_{K\times\mathbb{R}^2} vf\nabla_x\phi \right) = \frac{1}{k_n} \sum_{K\in\mathcal{T}_h} \int_{K\times\mathbb{R}^2} Q(f)\phi, \tag{3.2}$$

for all test functions $\phi \in V_{h,N}$. In the above equation, n is the unit length outer normal vector to the spatial element K.
For the discretization of the transport operator it is useful to interpret it as a standard linear transport operator in $\mathbb{R}^4$. This is achieved by introducing the new variable $y := (x,v) \in \mathbb{R}^4$, the wind vector $b := (v,0) \in \mathbb{R}^4$, the new domain $\widetilde{\Omega} := \Omega \times \mathbb{R}^2$ resp. mesh $\widetilde{\mathcal{T}_h} := \prod_{K\in\mathcal{T}_h} K \times \mathbb{R}^2$ and the outer normal vector to an element of $\widetilde{\mathcal{T}_h}$ by $\tilde{n} := (n,0)$. It is easy to see, that $\mathrm{div}_x(vf) = \mathrm{div}_y(bf)$, $b\cdot\tilde{n} = v\cdot n$ and that

$$\int_{K\times\mathbb{R}^2} \mathrm{div}_y(bf)\phi\, dy = \int_{\partial(K\times\mathbb{R}^2)} b\cdot\tilde{n} f\phi\, dy - \int_{K\times\mathbb{R}^2} b\cdot\nabla_y\phi f\, dy.$$

The resulting domain term can be treated by standard methods. For the boundary part, more work is needed. Since we have not excluded discontinuities along the boundary of $K\times\mathbb{R}^2$ it is – as in the lower dimensional case – not a priori clear, how to evaluate the boundary term. To solve this, an upwind discretization is applied, resulting in a different but – due to continuity of the exact solution – consistent formulation for the transport term:

$$\int_{K\times\mathbb{R}^2} \mathrm{div}_y(bf)\phi\, dy = \int_{\partial(K\times\mathbb{R}^2)} b\cdot\tilde{n} f^{\mathrm{up}}\phi\, dy - \int_{K\times\mathbb{R}^2} b\cdot\nabla_y\phi f\, dy$$

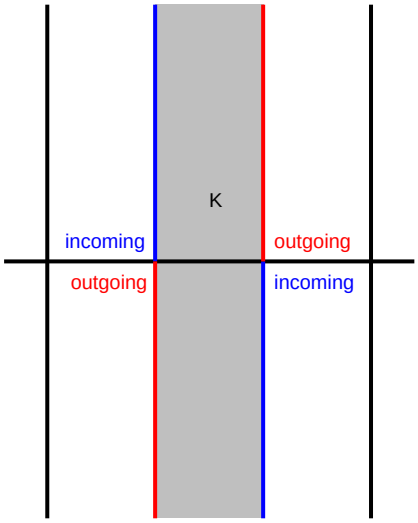

Fig. 1: Sketch for a $1d \times 1d$ situation, where $\Omega \subset \mathbb{R}$ and the momentum space is also restricted to $\mathbb{R}$. The grey shaded domain is the actual element of interest $K \times \mathbb{R}$. In the upper half of the plane are the positive velocities, the negative ones in the lower part. The incoming boundary part consists of those $(x, v) : n(x) \cdot v < 0$, while the points (x, v) on the outgoing part satisfy $n(x) \cdot v \geq 0$, $\forall\ (x, v) \in \partial K$. Consequently a particle on the incoming part of the boundary is transported to the inside of the element $K \times \mathbb{R}$ and vice versa for particles on the outgoing parts, justifying the notation "incoming" and "outgoing". In context of the upwind function f^{up}, this means to choose $f|_K$ for the outgoing parts and $f|_{K'}$ for the incoming parts.

with the upwind flux

$$f^{\text{up}} := \begin{cases} f\big|_K & \text{where } \langle b, \tilde{n} \rangle \geq 0 \\ f\big|_{K'} & \text{where } \langle b, \tilde{n} \rangle < 0 \end{cases},$$

with K' being the corresponding neighbour element to K.
The definition of the upwind flux is also sketched in figure 1:

The above definition of the upwind function holds for inner edges of the mesh $\mathcal{T}_h$ only. For a boundary edge the upwind value f^{up} has to be adjusted, instead of the solution value from the neighbouring element, the boundary value is used. For an inflow boundary condition (2.4c) this ends up in:

$$f^{\text{up}} := \begin{cases} f\big|_K & \text{where } \langle b, n \rangle \geq 0 \\ f_{\text{in}} & \text{where } \langle b, n \rangle < 0 \end{cases},$$

while for the specular reflection (2.4a) obtains:

$$f^{\text{up}} := \begin{cases} f\big|_K & \text{where } \langle b, n \rangle \geq 0 \\ f(v - 2\langle n, v \rangle n) & \text{where } \langle b, n \rangle < 0 \end{cases}.$$

This simple treatment of boundary conditions is a result of the nature of the boundary conditions, since they are only imposed for velocities in $\mathbb{R}^2_{\text{in}}$. With the expansion $f(t, x, v) = \sum_{j=1}^{\text{ndof}} c_j(t) f_j(x, v)$, where $\{f_j, j = 1 \dots \text{ndof}\}$ is a basis for $\widetilde{V}_{h,N}$ and testing with ϕ_j, with $\{\phi_j, j = 1 \dots \text{ndof}\}$ a basis for the test space yields:

$$M_h \frac{\partial c}{\partial t}(t) + A_h c(t) = \frac{1}{k_n} Q_h(c(t)) \tag{3.3}$$

with the mass matrix M_h, A_h denoting the discretization of the transport term and Q_h denotes the application of the collision operator to the discrete solution function.

This is an ODE system for the unknown coefficient vector c. Applying a forward euler scheme, denoting by $c^n \approx c(t_n), n = 0 \dots N_{t_{\text{end}}}$ and c^0 given results in:

$$c^{n+1} = c^n + \Delta_{t_n} M_h^{-1}(\frac{1}{k_n} Q_h(c^n) - A_h c^n), \tag{3.4}$$

with time step $\Delta t_n = t_{n+1} - t_n$. A similiar discrete time stepping procedure occurs when using higher order Runge Kutta methods instead. When using these schemes, typically the inverse of the mass matrix is needed for calculating c^{n+1}. Thus, we look for a basis of $V_{h,N}$ resp. $\widetilde{V}_{h,N}$, generating a sparse mass matrix. This basis is discussed in detail in [16]. We summarize the main ideas and properties:
In the velocity space a Lagrangian basis with collocation nodes x_{ip} is chosen. The nodes arise from a Gauss-Hermite quadrature rule $(x_{\text{ip}}, \omega_{\text{ip}})$, $i = 0 \dots N-1$, satisfying $\int_{\mathbb{R}} e^{-v^2} p(v) = \sum_{\text{ip}} \omega_{\text{ip}} p(x_{\text{ip}}),\ \forall p \in P^{2N-1}(\mathbb{R})$. N is directly related to the maximum partial polynomial degree in the space V^N. These Lagrange polynomials are denoted by $l_j, j = 0 \dots N$, and as already described, are multiplied with an appropriate Maxwellian. The $2-d$ bases arise by forming the tensor product of the $1-d$ Lagrange Polynomials. These multivariate basis polynomials are denoted by $L_j, j = 1 \dots \text{ndof}_v$. Using the properties of L_j and also of the quadrature rule one easily finds:

$$\int_{\mathbb{R}^2} e^{-|\frac{v-\overline{V}_K}{\sqrt{\overline{T}_K}}|^2} L_m(\tfrac{v-\overline{V}_K}{\sqrt{\overline{T}_K}}) L_n(\tfrac{v-\overline{V}_K}{\sqrt{\overline{T}_K}})\, dv = \overline{T}_K \delta_{m,n} \omega_n := (M_V)_{n,m}$$

Moreover, there also holds:

$$\int_{\mathbb{R}^2} v e^{-|\frac{v-\overline{V}_K}{\sqrt{\overline{T}_K}}|^2} L_m(\tfrac{v-\overline{V}_K}{\sqrt{\overline{T}_K}}) L_n(\tfrac{v-\overline{V}_K}{\sqrt{\overline{T}_K}})\, dv = v_n \overline{T}_K \delta_{m,n} \omega_n,$$

To keep orthogonality of the basis, for a given $\overline{V}_K$ and $\overline{T}_K$, the polynomials are scaled and shifted in the argument:

$$V_N = \text{span}\{L_j(\frac{v - \overline{V}_K}{\sqrt{\overline{T}_K}}), j = 0 \dots (N+1)^2 - 1\} \tag{3.5}$$

Denoting the spatial basis polynomials in a single element K by $\{u_r, r = 1 \dots \text{ndof}_x\}$ and testing against $\phi = L_n(v) u_{r'}(x)$ results in:

$$\begin{aligned}
\int_{K \times \mathbb{R}^2} f(t,x,v)\phi(x,v) d(x,v) &= \sum_{r=1}^{\text{ndof}_x} \sum_{m=1}^{\text{ndof}_v} c_{r,m} \int_K u_r(x) u_{r'}(x)\, dx \times \\
&\quad \int_{\mathbb{R}^2} e^{-|\frac{v-\overline{V}_K}{\sqrt{\overline{T}_K}}|^2} L_m(\tfrac{v-\overline{V}_K}{\sqrt{\overline{T}_K}}) L_n(\tfrac{v-\overline{V}_K}{\sqrt{\overline{T}_K}})\, dv \\
&= \overline{T}_K \sum_{r=1}^{\text{ndof}_x} c_{r,n} \omega_n \int_K u_r(x) u_{r'}(x)\, dx.
\end{aligned}$$

Denoting $c^K = (c^K_{1,1}, \dots, c^K_{1,\text{ndof}_v}, \dots, c^K_{\text{ndof}_x,1}, \dots, c^K_{\text{ndof}_x,\text{ndof}_v-1})$ the coefficients for the element K, the total mass matrix M_K for a single element K is the Kronecker product $M_K = M_x \otimes M_V \in \mathbb{R}^{\text{ndof}_x \text{ndof}_v \times \text{ndof}_x \text{ndof}_v}$, with the spatial mass matrix $(M_x)_{i,j} := \int_K u_j(x) u_i(x)\, dx$. The global matrix M_h is therefore a block diagonal

matrix and can easily be inverted.

REMARK 3.1. *For tetrahedron elements K, also the spatial basis functions u_r satisfy $\int_K u_r u_{r'}\,dx = c_r\delta_{r,r'}$, such that for the resulting block $(M_K)_{i,j} = \tilde{c}_j\delta_{i,j}$.*

4. Application of the collision integrals. A crucial part of the scheme is the application of the collision integrals (this is not due to the discretization scheme but to the collision operator itself). For a given distribution function f and a fixed spatial point the evaluation of the operator takes $O(N^4)$ operations. We consider a fixed element in the mesh $\mathcal{T}_h$. For a spatial position x and a time t there holds $Q(f)(t,x,v) = Q(f(t,x,.))(v)$ such that Q acts pointwise in position and time, but global in velocity. For the collision integrals inside the element $\tilde{K} = K \times \mathbb{R}^2 \in \widetilde{\mathcal{T}_h}$ one obtains:

$$\int\limits_{K\times\mathbb{R}^2} Q(f)(t,x,v)\phi(v)\,dv\,dx = \int\limits_K \underbrace{\left(\int\limits_{\mathbb{R}^2} Q(f(t,x,.))(v)\phi(x,v)\,dv\right)}_{:=g(x)} dx = \sum_{\text{ip}} \omega_{\text{ip}} g(x_{\text{ip}}),$$

with the pair $(x_{\text{ip}}, \omega_{\text{ip}})$ being an integration rule on the element K, such that $\int_K p(x)\,dx = \sum_{\text{ip}} \omega_{\text{ip}} p(x_{\text{ip}})\ \forall p \in V_h$. Substituting $\frac{v-\overline{V}_K}{\sqrt{\overline{T}_K}} =: \tilde{v}$ resp. $\frac{w-\overline{V}_K}{\sqrt{\overline{T}_K}} =: \tilde{w}$ gives for the post collision velocities:

$$\begin{aligned} v' &= \frac{\sqrt{\overline{T}_K}\tilde{v} + \overline{V}_K + \sqrt{\overline{T}_K}\tilde{w} + \overline{V}_K}{2} + \sqrt{\overline{T}_K}e'\frac{|\tilde{v}-\tilde{w}|}{2} = \sqrt{\overline{T}_K}\tilde{v}' + \overline{V}_K \\ w' &= \frac{\sqrt{\overline{T}_K}\tilde{v} + \overline{V}_K + \sqrt{\overline{T}_K}\tilde{w} + \overline{V}_K}{2} - \sqrt{\overline{T}_K}e'\frac{|\tilde{v}-\tilde{w}|}{2} = \sqrt{\overline{T}_K}\tilde{w}' + \overline{V}_K \end{aligned} \tag{4.1}$$

Combining (2.2),(4.1) and introducing the normalized distribution $f^{0,1}(t,x,v) := f(t,x,\sqrt{\overline{T}_K}v + \overline{V}_K)$, g simplifies to

$$\begin{aligned} \int\limits_{\mathbb{R}^2} Q(f)\phi\,dv &= \int\limits_{\mathbb{R}^2}\int\limits_{\mathbb{R}^2}\int\limits_{S^1} B(v,w,e')[f(t,x,v')f(t,x,w') - f(t,x,v)f(t,x,w)]\phi(x,v)\,dv \\ &= \overline{T}_K^{2+\frac{\beta}{2}} \int\limits_{\mathbb{R}^2}\int\limits_{\mathbb{R}^2}\int\limits_{S^1} b_r(|v-w|)b_\theta(\tfrac{(v-w)\cdot e'}{|v-w|})\times \\ &\qquad [f^{0,1}(t,x,v')f^{0,1}(t,x,w') - f^{0,1}(t,x,v)f^{0,1}(t,x,w)]\phi^{0,1}(x,v)\,dv \\ &= \overline{T}_K^{2+\frac{\beta}{2}} \int\limits_{\mathbb{R}^2} Q(f^{0,1})\phi^{0,1}\,dv. \end{aligned} \tag{4.2}$$

For the discrete solution $f_{h,N} \in \widetilde{V}_{h,N}$ at a fixed spatial position x_0 one obtains

$$f_{h,N}(t,x_0,v) = e^{-\left|\frac{v-\overline{V}_K}{\sqrt{\overline{T}_K}}\right|^2} \sum_m \underbrace{\sum_r c_{r,m}u_r(x_0)}_{:=c_m^{x_0}} L_m(\tfrac{v-\overline{V}_K}{\sqrt{\overline{T}_K}}), \tag{4.3}$$

respectively, $f^{0,1}_{h,N}(t,x_0,v) = e^{-|v|^2}\sum_m c^{x_0}_m L_m(v)$.
Finally, combining conservation of energy during a binary collision (i.e. $|v|^2+|w|^2 = |v'|^2+|w'|^2$), (4.2) and the above expansion, g results in ($\phi = u_r(x)L_k(\frac{v-\overline{V}_K}{\sqrt{\overline{T}_K}})$):

$$g(x_{\mathrm{ip}}) = u_r(x_{\mathrm{ip}})\overline{T}_K^{2+\frac{\beta}{2}} \sum_{m,n} c^{x_{\mathrm{ip}}}_m c^{x_{\mathrm{ip}}}_n \times \int_{\mathbb{R}^2}\int_{\mathbb{R}^2}\int_{S^1} b_r b_\theta e^{-|v|^2-|w|^2}\left[L_m(v')L_n(w') - L_m(v)L_n(w)\right] L_k(v)\, de'\, dv\, dw.$$

For the sake of simplicity in the above formula, the dependency of b_r and b_θ on their arguments has been omitted. The evaluation of the collision integrals is independent from the current macroscopic velocity $\overline{V}_K$. The dependency on the temperature reduces to a simple multiplication with $\overline{T}_K^{2+\beta/2}$.
Now consider the mapping $G : (c^{x_{\mathrm{ip}}}_1 c^{x_{\mathrm{ip}}}_1, c^{x_{\mathrm{ip}}}_1 c^{x_{\mathrm{ip}}}_2, \ldots, c^{x_{\mathrm{ip}}}_{\mathrm{ndof}} c^{x_{\mathrm{ip}}}_{\mathrm{ndof}}) \mapsto g(x_{\mathrm{ip}}) \in \mathbb{R}^{\mathrm{ndof}}$, which is obviously linear in it' s $(N+1)^4$ arguments. Due to linearity, G is a matrix-vector multiplication, resulting in $O(N^6)$ floating point operations for evaluation. To calculate the collision integrals in an efficient way we will now briefly recapitulate the techniques introduced in [16]:
If not explicitly declared, the t and x dependency of f is omit for the rest of the section due to readability. Due to (4.2) we can restrict ourselves to the case $\overline{V}_K = 0$, $\overline{T}_K = 1$, the general case is then obtained by multiplying the result with $\overline{T}_K^{2+\beta/2}$. Remark, that the coefficients describing $f_{h,N}$ resp. $f^{0,1}_{h,N}$ coincide, and therefore no effort for calculating $f^{0,1}_{h,N}$ is needed.

Step 1:

First of all we make use of a different representation for $\int_{\mathbb{R}^2} Q(f)\phi\, dv$:

(4.4)

$$\begin{aligned}\int_{\mathbb{R}^2} Q(f(v))\phi(v)\, dv &= \int_{\mathbb{R}^2}\int_{\mathbb{R}^2}\int_{S^1} B(v,w,e')f(v)f(w)[\phi(v') - \phi(v)]\, de'\, dw\, dv \\ &= \frac{1}{2}\int_{\mathbb{R}^2}\int_{\mathbb{R}^2}\int_{S^1} B(v,w,e')f(v)f(w)\times \\ &\qquad [\phi(v') + \phi(w') - \phi(v) - \phi(w)]\, de'\, dw\, dv \\ &= \frac{1}{4}\int_{\mathbb{R}^2}\int_{\mathbb{R}^2}\int_{S^1} B(v,w,e')[f(v)f(w) - f(v')f(w')]\times \\ &\qquad [\phi(v') + \phi(w') - \phi(v) - \phi(w)]\, de'\, dw\, dv\end{aligned}$$

A proof for the above statement can be found in [15].
We start with the first equal representation in (4.4) and subsitute $\bar{v} := \frac{v+w}{2}$, $\hat{v} := \frac{v-w}{2}$. Moreover we define $f^{\bar{v}}(\hat{v}) := f(\bar{v}+\hat{v})$. This leads to

$$\int_{\mathbb{R}^2} Q(f(v))\phi(v)\, dv = 4\int_{\mathbb{R}^2}\int_{\mathbb{R}^2}\int_{S^1} b_r(|\hat{v}|)b_\theta(\tfrac{\hat{v}\cdot e'}{|\hat{v}|})f^{\bar{v}}(\hat{v})f^{\bar{v}}(-\hat{v})[\phi^{\bar{v}}(e'|\hat{v}|) - \phi^{\bar{v}}(\hat{v})]\, de' d\hat{v}\, d\bar{v}$$

Finally, letting $f_2^{\bar{v}}(\hat{v}) := f^{\bar{v}}(\hat{v}) f^{\bar{v}}(-\hat{v})$, one arrives with

$$\int_{\mathbb{R}^2} Q(f(v))\phi(v)\,dv = 4 \underbrace{\int_{\mathbb{R}^2} \int_{\mathbb{R}^2} \int_{S^1} b_r(|\hat{v}|) b_\theta(\tfrac{\hat{v}\cdot e'}{|\hat{v}|}) f_2^{\bar{v}}(\hat{v}) [\phi^{\bar{v}}(e'|\hat{v}|) - \phi^{\bar{v}}(\hat{v})]\,de' d\hat{v}\; d\bar{v}}_{:= Q^I(b_r f_2^{\bar{v}}, \phi^{\bar{v}})(\bar{v})}.$$

For a given function $f_{h,N} \in \widetilde{V}_{h,N}$, the argument shifted function $f^{\bar{v}}(\hat{v})$ can be evaluated within $O(N^3)$ operations. $f_2^{\bar{v}}$ results in a polynomial of degree $2N$, multiplied with a Maxwellian with temperature $\frac{1}{2}$. As presented in [16], the computational effort for $f_2^{\bar{v}}$, is also bounded by $O(N^3)$. The key idea to obtain this bound is to already approximate $f^{\bar{v}}$ by Lagrange polynomials of degree $2N$. This of course increases the computational effort for $f^{\bar{v}}$, but also bounds it by $O(N^3)$.

The calculation of $\tilde{f}_2^{\bar{v}} := b_r f_2^{\bar{v}}$ is done at this point of the calculations, resulting in a point-wise multiplication of the coefficients of $f_2^{\bar{v}}$ with the values of $b_r(|\hat{v}|)$. In the sequel, the tilde sign is removed, and we denote by $f_2^{\bar{v}}$ the above mentioned function $\tilde{f}_2^{\bar{v}}$.

Step 2:

The next step is to replace the integration with respect to $\bar{v}$ by a Gauss-Hermite quadrature rule, resulting in:

$$\int_{\mathbb{R}^2} Q(f(v))\phi(v)\,dv = 2 \sum_{\mathrm{ip}=1}^{n_{\mathrm{ip}}} \omega_{\mathrm{ip}} Q^I(f_2^{\frac{\bar{v}_{\mathrm{ip}}}{\sqrt{2}}}, \phi^{\frac{\bar{v}_{\mathrm{ip}}}{\sqrt{2}}})(\frac{\bar{v}_{\mathrm{ip}}}{\sqrt{2}}) \tag{4.5}$$

In the above equation, the pair $(\bar{v}_i, \omega_i)$, $i = 1 \dots n_{\mathrm{ip}}$ is a Gauss-Hermite integration formula. The additional scaling of the quadrature nodes by $1/\sqrt{2}$ is to obtain a Maxwellian with temperature 1 in the integrand, since for such integrands, the Gauss-Hermite quadrature rule fits perfect. At this point, the computational effort is bounded by the number n_{ip} of integration points w.r.t. $\bar{v}$, multiplied with the computational effort for evaluating $Q^I(f)$. Since Q^I is linear in $f_2^{\bar{v}}$, its evaluation is a matrix-vector multiplication of size $N^2 \times 4N^2$, resulting in $O(N^4)$ operations. This gives a total complexity of $O(N^4) n_{\mathrm{ip}}$. Finally we consider the application of the inner collision operator Q^I:

Step 3:

This step is carried out by a basis transformation in the momentum space for $f_2^{\bar{v}}$. The basis in which Q^I is applied, is given in Polar coordinates. To transform from the nodal to the Polar basis in an efficient way, we introduce an additional polynomial basis to reduce computational effort. By $H_n(v)$ we denote the n-th (scaled) $1d$-Hermite polynomial. These are orthonormal w.r.t. $\langle f, g\rangle = \int_{\mathbb{R}} e^{-v^2} f g\,dv$ [17]. In addition by $\mathcal{L}_n^\alpha$ we denote the (scaled) generalized n-th Laguerre polynomial. These are orthonormal w.r.t. $\langle f, g\rangle = \int_{\mathbb{R}^+} v^\alpha e^{-v} f g\,dv$ [17]. The resulting two dimensional bases we use are a hierarchical basis consisting of the Hermite polynomials:

$$\mathcal{H}_{m,n}(v) := H_m(v_x) H_{m-n}(v_y) \qquad n \le m,\ m = 0 \dots 2N, \tag{4.6}$$

and in addition the Polar polynomials which are given by:

(4.7)

$$\Psi^{\cos}_{j,k}(v) := \begin{cases} s_{j,k}\cos(2j\varphi)r^{2j}\mathcal{L}^{(2j)}_{\frac{k}{2}-j}(r^2), & k \in 2\mathbb{N},\ j = 0\dots k/2 \\ s_{j,k}\cos((2j+1)\varphi)r^{2j+1}\mathcal{L}^{(2j+1)}_{\frac{k-1}{2}-j}(r^2), & k \in 2\mathbb{N}+1,\ j = 0\dots \lfloor k/2 \rfloor \end{cases}$$

and

$$\Psi^{\sin}_{j,k}(v) := \begin{cases} s_{j,k}\sin(2j\varphi)r^{2j}\mathcal{L}^{(2j)}_{\frac{k}{2}-j}(r^2), & k \in 2\mathbb{N},\ j = 1\dots k/2 \\ s_{j,k}\sin((2j+1)\varphi)r^{2j+1}\mathcal{L}^{(2j+1)}_{\frac{k-1}{2}-j}(r^2), & k \in 2\mathbb{N}+1,\ j = 0\dots \lfloor k/2 \rfloor \end{cases}$$

with (r,φ) the Polar coordinates of the velocity v, and $s_{j,k}$, being normalization constants for the angular part, i.e.: $s_{0,2k} = \sqrt{\frac{2}{\pi}}$, $s_{j,k} = \sqrt{\frac{1}{\pi}}$ in all other cases. In [16] it is shown that the polynomial spaces $\operatorname{span}\{\mathcal{H}_{m,n},\ m \le N,\ n \le m\} = \operatorname{span}\{\Psi^{\theta}_{j,k},\ k \le N,\ j \le \lfloor k/2 \rfloor, \theta \in \{\cos, \sin\}\}$ coincide.

LEMMA 4.1. *Let $S, S_0 \in \{\sin, \cos\}, 0 \le k \le N, 0 \le j \le \lfloor \frac{k}{2} \rfloor$. Then, the Polar polynomials satisfy $Q^I(e^{-|.|^2}\Psi^{S}_{j,k}, \Psi^{S_0}_{j_0,k_0})(\frac{\bar{v}}{\sqrt{2}}) = -\frac{1}{2}b_{S_0,k_0,j_0}\delta_{j,j_0}\delta_{k,k_0}\delta_{S,S_0}$ such that the inner collision operator Q^I applied in the Polar basis, is diagonal. b_{S_0,k_0,j_0} is given by*

$$b_{S_0,k_0,j_0} = \begin{cases} \int_0^{2\pi} b_\theta(\cos(\alpha))(1 - S_0(2j_0\alpha))\,d\alpha & k_0 \in 2\mathbb{N} \\ \int_0^{2\pi} b_\theta(\cos(\alpha))(1 - S_0((2j_0+1)\alpha))\,d\alpha & k_0 \in 2\mathbb{N}+1 \end{cases}$$

Proof. For simplicity we consider the case of $S = S_0 = \cos$ and k, k_0 even. In addition we let $j, j_0 > 0$.

$$Q^I(e^{-|.|^2}\Psi^{\theta}_{j,k}, \Psi^{\theta_0}_{j_0,k_0}) \overset{\hat{v}=r\,e}{=} \int_{\mathbb{R}^+}\int_{S^1}\int_{S^1} b_\theta(e\cdot e')e^{-r^2} r\Psi^{\theta}_{j,k}(r\,e)\times \left[\Psi^{\theta_0}_{j_0,k_0}(r\,e') - \Psi^{\theta_0}_{j_0,k_0}(r\,e)\right] de\,de'\,dr \tag{4.8}$$

The inner product of $e \cdot e'$ results in $\cos(\alpha - \alpha')$ within the usual parametrization of the unit spheres.

(4.9)

$$Q^I(e^{-|.|^2}\Psi^{\theta}_{j,k}, \Psi^{\theta_0}_{j_0,k_0}) = -\underbrace{s_{j_0,k_0}s_{j,k}}_{=\frac{1}{\pi}}\int_{\mathbb{R}^+} e^{-r^2} r r^{2j_0} r^{2j}\mathcal{L}^{(2j)}_{\frac{k}{2}-j}(r^2)\mathcal{L}^{(2j_0)}_{\frac{k_0}{2}-j_0}(r^2)\,dr\times \int_0^{2\pi}\int_0^{2\pi} b_\theta(\cos(\alpha-\alpha'))\cos(2j\alpha')\left[\cos(2j_0\alpha') - \cos(2j_0\alpha)\right]\,d\alpha\,d\alpha'$$

Now by the substitution $\alpha^{\Delta} = \alpha - \alpha'$, the two innermost integrals result in:

$$\frac{1}{\pi}\int_0^{2\pi}\int_0^{2\pi} b_\theta(\cos(\alpha-\alpha'))\cos(2j\alpha')\left[\cos(2j_0\alpha') - \cos(2j_0\alpha)\right]\,d\alpha\,d\alpha'$$

$$= \frac{1}{\pi} \int_0^{2\pi} \int_0^{2\pi} b_\theta(\cos(\alpha^\Delta)) \cos(2j(\alpha - \alpha^\Delta)) \left[\cos(2j_0(\alpha - \alpha^\Delta)) - \cos(2j_0\alpha)\right] d\alpha \, d\alpha^\Delta$$

(4.10)

$$= \delta_{j,j_0} \underbrace{\int_0^{2\pi} b_\theta(\cos(\alpha^\Delta))(1 - \cos(2j_0\alpha)) \, d\alpha^\Delta}_{:= b_{\cos,k_0,j_0}}$$

Thus, the inner collision operator results in:

(4.11)

$$- \delta_{j,j_0} b_{\cos,k_0,j_0} \int_{\mathbb{R}^+} e^{-r^2} r r^{4j_0} \mathcal{L}^{(2j_0)}_{\frac{k}{2}-j_0}(r^2) \mathcal{L}^{(2j_0)}_{\frac{k_0}{2}-j_0}(r^2) \, dr$$

$$\overset{r=\sqrt{\bar{r}}}{=} -\frac{1}{2} \delta_{j,j_0} b_{\cos,k_0,j_0} \underbrace{\int_{\mathbb{R}^+} e^{-r} r^{2j_0} \mathcal{L}^{(2j_0)}_{\frac{k}{2}-j_0}(r) \mathcal{L}^{(2j_0)}_{\frac{k_0}{2}-j_0}(r) \, dr}_{=\delta_{k,k_0}} =$$

(4.12)

$$= -\frac{1}{2} \delta_{j,j_0} \delta_{k,k_0} b_{\cos,k_0,j_0}$$

The other cases are quite similar to obtain. □

REMARK 4.2. *Obviously, the polynomial spaces for $f_2^{\bar{v}}$, V_{2N}=span$\{x^i y^j,\ i,j = 0 \dots 2N\}$ and* span$\{\mathcal{H}_{m,n},\ n \le m,\ m = 0 \dots 2N\}$ *do not coincide (The first one is of partial order $2N$, the latter is of total order $2N$). At least total order $4N$ is necessary to have $f_2^{\bar{v}}$ exact. A degree of $2N$ is needed for the test functions. Therefore, we choose the Polar test space of order $2N$. Using lemma 4.1, the collision integrals vanish for all Polar trial functions of order greater than $2N$. Thus, having in mind the hierarchical structure of the Polar basis, a transformation of $f_2^{\bar{v}}$ to order $2N$ is sufficient.*

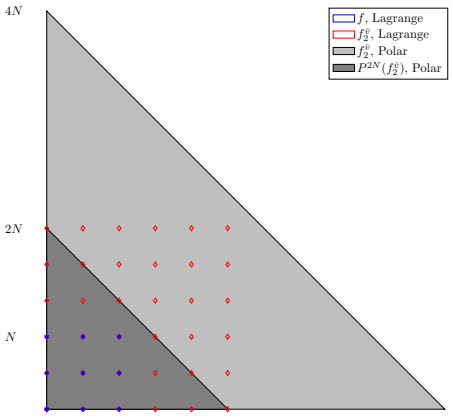

Fig. 2: The markers are the polynomial coefficients in v_x resp. v_y direction. The gray shaded domains are the coefficients in the hierarchical basis. The lighter one corresponds to an exact representation of $f_2^{\bar{v}}$ in a polar basis with order $4N$, the darker one corresponds to an inexact representation of $f_2^{\bar{v}}$ but still to an exact $\int_{\mathbb{R}^2} Q(f)\phi \, dv$. The darker coefficients correspond to the L_2-orthogonal projection of $f_2^{\bar{v}}$ to the space span$\{\mathcal{H}_{m,n},\ n \le m, m = 0 \dots 2N\}$.

LEMMA 4.3. *The above introduced polynomial bases $\{\mathcal{H}_{m,n} : n \le m, m \le 2N\}$ and $\{\Psi^{\cos}_{j,k} : k \le 2N, j \le \lfloor \frac{k}{2} \rfloor\} \cup \{\Psi^{\sin}_{j,k} : k \le 2N, I_{2\mathbb{N}}(k) \le j \le \lfloor \frac{k}{2} \rfloor\}$ are orthogonal*

w.r.t. the weighted L_2-inner product $\langle f, g\rangle = \int_{\mathbb{R}^2} e^{-|v|^2} f g \, dv$. $I_M(x)$ denotes the indicator function to the set M evaluated at x.

Proof. The calculations are straightforward for the Hermite basis:

$$\begin{aligned}\int_{\mathbb{R}^2} e^{-|v|^2} \mathcal{H}_{m,n}(v)\mathcal{H}_{m_0,n_0}(v)\,dv &= \int_{\mathbb{R}} e^{-v_x^2} H_m(v_x)H_{m_0}(v_x)\,dv_x \times \\ &\quad \int_{\mathbb{R}} e^{-v_y^2} H_{m-n}(v_y)H_{m_0-n_0}(v_y)\,dv_y \\ &= \delta_{m,m_0}\delta_{m-n,m_0-n_0} = \delta_{m,m_0}\delta_{n,n_0}\end{aligned} \tag{4.13}$$

For the Polar basis the situation is more complex. Transforming the integrals to Polar coordinates and additionally substituting $r^2 = \tilde{r}$ one obtains the same statement for the Polar basis:

$$\begin{aligned}\int_{\mathbb{R}^2} e^{-|v|^2} \Psi^{\alpha}_{j,k}(v)\Psi^{\beta}_{j_0,k_0}(v)\,dv &= \int_{\mathbb{R}^+}\int_{S^2} r e^{-r^2} \Psi^{\alpha}_{j,k}(re')\Psi^{\beta}_{j_0,k_0}(re')\,de'\,dr = \\ &= \delta_{\alpha,\beta}\delta_{j,j_0} \int_{\mathbb{R}^+} r e^{-r^2} r^{4j_0+2} \mathcal{L}^{(2j_0+1)}_{\frac{k-1}{2}-j_0}(r^2)\mathcal{L}^{(2j_0+1)}_{\frac{k_0-1}{2}-j_0}(r^2)\,dr \\ &= \delta_{j,j_0}\delta_{k,k_0}\delta_{\alpha,\beta}.\end{aligned} \tag{4.14}$$

The red numbers are only present when k and k_0 are odd. □

The orthogonality w.r.t. the same inner product is the key ingredient when transforming from Hermite to Polar polynomials in an efficient way, since it is the reason for sparse transformation operations.

Now we transform $f_2^{\bar{v}}$ given by its nodal representation to the Hermite basis and finally to the Polar basis in which the inner collision operator is applied. Both transformations are bounded by $O(N^3)$ operations.

Transformation to Hermite:

We start with the first transformation from the Lagrange basis to the Hermite basis. Let $f_2^{\bar{v}} = e^{-2|v|^2}\sum_m c_m L_m(v)$. For the coefficients in Hermitian basis we require

$$\sum_m c_m \int_{\mathbb{R}^2} e^{-2|v|^2} L_m(v)\mathcal{H}_{k_0,j_0}(\sqrt{2}v)\,dv = \sum_{\substack{j=0\dots k\\ k=0\dots 2N}} h_{k,j} \int_{\mathbb{R}^2} e^{-2|v|^2}\mathcal{H}_{k,j}(\sqrt{2}v)\mathcal{H}_{k_0,j_0}(\sqrt{2}v)\,dv, \tag{4.15}$$

for all test polynomials in $\operatorname{span}\{\mathcal{H}_{m,n},\ n \le m,\ m = 0\dots 2N\}$. Due to orthogonality, the right hand side turns into $\frac{1}{2}h_{k_0,j_0}$. The left hand side turns into a matrix vector multiplication $M\cdot c$, with $M_{n,m} = \int_{\mathbb{R}^2} e^{-2|v|^2} L_m(v)\mathcal{H}_{j,k}(\sqrt{2}v)\,dv$, where $n = \frac{k(k+1)}{2}+j$. This matrix vector product is of computational effort $O(N^4)$.

Since both bases contain a tensor product structure, this matrix vector product can be factorized, resulting in a matrix-matrix-matrix product, reducing computational effort to $O(N^3)$. The resulting operation is a separated transformation in the v_x-direction first and the v_y-direction afterwards.

Transformation to Polar:

To conserve mass, momentum and energy the transformation is in the sense of an

orthogonal projection:

$$\sum_{\substack{m\le 2N\\ n\le m}} h_{m,n}\int_{\mathbb{R}^3} e^{-2|v|^2}\mathcal{H}_{m,n}(\sqrt{2}v)\Psi^{S_0}_{j_0,k_0}(\sqrt{2}v)\,dv = \sum_{\substack{k\le 2N\\ j\le \lfloor k/2\rfloor\\ S\in\{\sin,\cos\}}} \psi_{j,k,S}\int_{\mathbb{R}^3} e^{-2|v|^2}\Psi^{a}_{j,k}(\sqrt{2}v)\Psi^{S_0}_{j_0,k_0}(\sqrt{2}v)\,dv, \tag{4.16}$$

with $S_0 \in \{\cos, \sin\}$. Due to the orthogonality of the Polar basis functions the right hand side of (4.16) turns into ψ_{j_0,k_0,S_0}. On the left hand side we split the sum into $\sum_{m\le 2N} = \sum_{m<k_0} + \sum_{m=k_0} + \sum_{m>k_0}$. For the first part we expand $\mathcal{H}_{m,n}$ to Polar polynomials, for the latter $\Psi^{S_0}_{j_0,k_0}$ is expanded to Hermite polynomials. Combining this with orthogonality, the first and third sum vanish. Thus, the coefficients in the Polar basis for a fixed total order k_0 depend only on those coefficients in the hermite basis of the same total polynomial order k_0. This gives a computational effort of $\sum_{k=0}^{2N}(k+1)^2 = \frac{(2N+1)(N+1)(8N+5)}{2} = O(N^3)$.

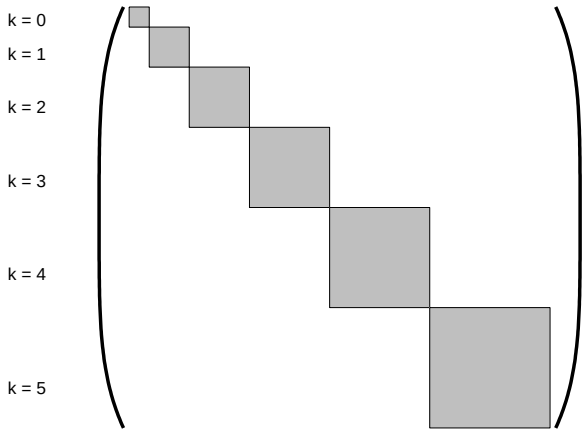

Fig. 3: The structure of the transformation matrix from the Hermite to the Polar basis, when sorting both bases hierarchical. The gray shaded blocks are the only non zero entries in the matrix. The $k-$th block is of size $(k+1)\times(k+1)$.

REMARK 4.4. *In addition to transform $f_2^{\bar{v}}$ to the Polar basis it is also necessary to transform the test functions from their Polar representation back to the nodal one. The transformation to the Hermite basis, the transformation from the Hermite to the nodal basis and also the back shifting of the test functions result in multiplications with the transposed matrices [16].*

5. Adaptive choice of element Maxwellians. A crucial part of the scheme is the choice of the quantities $\overline{V}(x)$ and $\overline{T}(x)$ describing the element Maxwellian. As a preparation we introduce the macroscopic quantities density ρ, bulk velocity V and

temperature T which are given below:

$$\begin{aligned} \rho(t,x) &:= \int_{\mathbb{R}^2} f(t,x,v)\,dv \qquad V(t,x) := \frac{1}{\rho(t,x)} \int_{\mathbb{R}^2} v f(t,x,v)\,dv \\ T(t,x) &:= \frac{1}{\rho(t,x)} \int_{\mathbb{R}^2} (v - V(t,x))^2 f(t,x,v)\,dv \end{aligned} \tag{5.1}$$

For good approximation properties the parameters $\overline{V}(x)$ and $\overline{T}(x)$ should be close to the macroscopic velocity $V(t,x)$ and temperature $T(t,x)$. We choose element wise constant $\overline{V} \in [P^0(\mathcal{T}_h)]^2$ and $\overline{T} \in P^0(\mathcal{T}_h) := \{u \in L_2(\Omega) \,:\, u\big|_K \equiv u_K,\ \forall K \in \mathcal{T}_h\}$. In addition we denote the mean value of a function $u \in L_2$ by $\frac{1}{|K|}\int_K u(x)\,dx =: \{u\}_K$, where $|K|$ is the volume of the element $K \in \mathcal{T}_h$. The jump of u along element boundaries is denoted by $[u]_{K,\tilde{K}}$, which is well defined for functions $u \in P^0(\mathcal{T}_h)$. A simple requirement for the parameters of the element Maxwellian is:

$$\overline{V}_K \equiv \overline{V}(t,x)\big|_K \equiv \{V(t,.)\}_K \quad \text{and} \quad \overline{T}_K \equiv \overline{T}(t,x)\big|_K \equiv \{T(t,.)\}_K \quad \forall K \in \mathcal{T}_h.$$

In practice this choice is not very useful, since it is unstable due to several reasons: The definition of the upwind function incorporates $f\big|_K$ as well as $f\big|_{\tilde{K}}$, with $\tilde{K}$ being a neighbour element to K. This gives need to a projection of the solution from one set of macroscopic Ansatz quantities to another. To give an idea of the problem let $L_{2,u} := \{f \in L_2(\mathbb{R}^2) : \int_{\mathbb{R}^2} e^{\frac{v^2}{u}} f(v)^2\,dv < \infty\}$. Now consider a discrete solution $f(v) = e^{-\frac{v^2}{T_0}} P(v)$, with $P \in P^k(\mathbb{R}^2)$ which has to be transferred to $\tilde{f}(v) = e^{-\frac{v^2}{T_1}} \tilde{P}(v)$. To have the orthogonal projection well defined, f has to be in L_{2,T_1}:

$$\int_{\mathbb{R}^2} e^{\frac{v^2}{T_1}} f(v)^2\,dv = \int_{\mathbb{R}^2} e^{v^2\left(\frac{1}{T_1} - \frac{2}{T_0}\right)} P(v)^2\,dv < \infty \Leftrightarrow T_0 < 2T_1 \tag{5.2}$$

Thus the projection is well defined if $T_0 < T_1$. The other way round, a restriction on the temperature T_1 is necessary to have the $L_{2,T_1}-$projection well defined. To overcome this problem – which also effects stability in actual computations – we bound the jumps of the temperature parameter $\overline{T}(t,x)$ by a constant $c < 2$. Moreover, we require it to be greater or equal than the mean of the macroscopic temperature defined in (5.1):

$$\overline{T} := \operatorname*{argmin}_{\substack{u \in P^0(\mathcal{T}_h) \\ u \geq \{T\} \\ [u] \leq c}} \|u(t,x) - \{T(t,x)\}\|_{L_2(\Omega)}\,. \tag{5.3}$$

The choice of the velocity parameter $\overline{V}(t,x)$ is motivated by the behaviour at the boundary. A perfect reflecting wall yields 0 normal component, diffuse reflection yields even 0 for the macroscopic velocity V. To incorporate this behaviour in the element Maxwellian, we solve the auxiliary $H(\mathrm{div})$ mass problem for $\overline{V}$:
Find $u \in H(\mathrm{div})(\Omega) := \{u \in [L_2(\Omega)]^2 : \mathrm{div} u \in L_2\}$, s.t.:

$$\sum_{K \in \mathcal{T}_h} \int_K u(x)\varphi(x)\,dx + \alpha \sum_{K \in \mathcal{T}_h} \int_K \mathrm{div}(u)(x)\mathrm{div}(\varphi)(x)\,dx = \sum_{K \in \mathcal{T}_h} \int_K V(t,x)\,dx \qquad \forall \varphi \in H(\mathrm{div})(\Omega) \tag{5.4}$$

The constant α is the penalty parameter, controlling how strong the solution is forced to attain the 0 normal component. For the solution of (5.4) on the discrete level, the lowest order Raviart Thomas space is chosen, which already contains linear polynomials. To have the Ansatz velocity in $[P^0(\mathcal{T}_h)]^2$, we project the discrete solution u_h of (5.4) onto $[P^0(\mathcal{T}_h)]^2$.

6. Numerical results. In this section we present numerical results as a validation for our method.

Example 1:
The first problem is a spatially homogeneous example, well known as the BKW solution [18, 4, 19], which is a non-stationary analytic solution of the spatially homogeneous Boltzmann equation $\frac{\partial f}{\partial t}(v) = Q(f)(v)$. In 2 dimensions it is given by:

$$f(t,v) = \frac{1}{2\pi s(t)} e^{-\frac{|v|^2}{2s(t)}} \left(1 - \frac{1-s(t)}{2s(t)}\left(2 - \frac{|v|^2}{s(t)}\right)\right), \tag{6.1}$$

with $s(t) = 1 - e^{-\frac{(t+t_0)}{8}}$.
The starting time t_0 is chosen such that $s(0) = \frac{1}{2}$ and thus, $f(0,v) = \frac{1}{\pi}|v|^2 e^{-|v|^2}$. Since $s \to 1$ if $t \to \infty$, the stationary solution is given by

$$f_\infty(v) = (2\pi)^{-1} e^{-\frac{|v|^2}{2}}, \tag{6.2}$$

which is a Maxwellian with temperature 2, velocity 0 and density 1.
Due to the conservation laws, f_∞ can also be obtained by calculating density, momentum and energy of $f(t,.)$ for any arbitrary t such that $f(t,.) \geq 0$, and then forming the Maxwellian corresponding to these macroscopic quantities. Figure 4 presents snapshots of the distribution function and the behaviour of the L_∞ norm on $(0, T_{\text{end}}$ of the L_2-error of the solution function.

Example 2:
The second example considers the flow around a cylinder. The geometry and the mesh for the computation are can be seen in figure 5. The boundary conditions on the cylinder and also on the upper and lower boundary of the computational domain are specular reflection (2.4b) with $T_{\text{bnd}} = 1$ and $V_{\text{bnd}} = (0,0)^T$. On the left and right side of the domain, the inflow condition (2.4c) is prescribed, where the function f_{in} is given in terms of Maxwellian distribution functions:

$$\begin{aligned} f_{\text{in}}(t,x,v) &= \frac{1}{2\pi T_{\text{in}}(x)} e^{-\left|\frac{v - V_{\text{in}}(x)}{\sqrt{T_{\text{in}}(x)}}\right|^2} \\ &\text{with} \\ V_{\text{in}}(x) &= \left(0, \frac{-1200x_2^2 + 60x_2 + 90}{121}\right) \\ T_{\text{in}}(x) &\equiv 1 \end{aligned} \tag{6.3}$$

This setting gives a quadratic inflow profile w.r.t the macroscopic velocity $V_2(x)$ with maximum inflow velocity 0.75. Since $V_2(0, 0.3) = V_2(0, -0.25) = 0$ the inflow profile fits well to the other boundary conditions. In order to have the initial condition consistent with the boundary conditions, the initial condition is chosen as

$$f_0(x,v) = f_{\text{in}}(x,v). \tag{6.4}$$

For an exact representation of the macroscopic quantities of the initial data and the inflow, a polynomial space of order 2 in the spatial domain is needed. Due to the coarse mesh this order was increased to 6, to resolve the solution accurate. The momentum order is 3, the time step is $\Delta t = 0.5 \cdot 10^{-3}$, combined with the improved euler method as a time stepping scheme. The mesh $\mathcal{T}_h$ consists of 141 spatial elements with polynomial trial functions of order 6. This gives a total number of degrees of freedom of $141 \cdot 28 \cdot 16 \approx 63000$. In figure 5, the modulus of the macroscopic velocity at different point in time are depicted. For the presented results, the knudsen number was chosen $k_n = 0.005$.

Example 3:
In this example the famous Mach 3 wind tunnel experiment is considered. The tunnel has a backward facing step at position $x = 0.6$ with height 0.2. The total length of the tunnel is 3 and its height is 1. The initial condition as well as the inflow is given in terms of Maxwellian Distribution functions, with desired macroscopic quantities:

$$\rho_0(x) \equiv 1.4, \qquad V_0(x) \equiv 3, \qquad T_0(x) \equiv 1,$$

such that – as in the previous example – the initial distribution is given by:

$$f_0(t,x,v) = \frac{1}{2\pi T_0} e^{-\left|\frac{v-V_0}{\sqrt{T_0}}\right|^2} \tag{6.5}$$

The mesh we use consists of 3772 spatial elements with order 3 trial and test polynomials in space. The order in momentum is 8 such the total number of degrees of freedom is $3772 \cdot 10 \cdot 81 \approx 3 \cdot 10^6$. The time step is $2.5 \cdot 10^{-5}$, the mean free path k_n was chosen $k_n = 0.0025$. Figure 6 depicts the macroscopic density at different points in time.

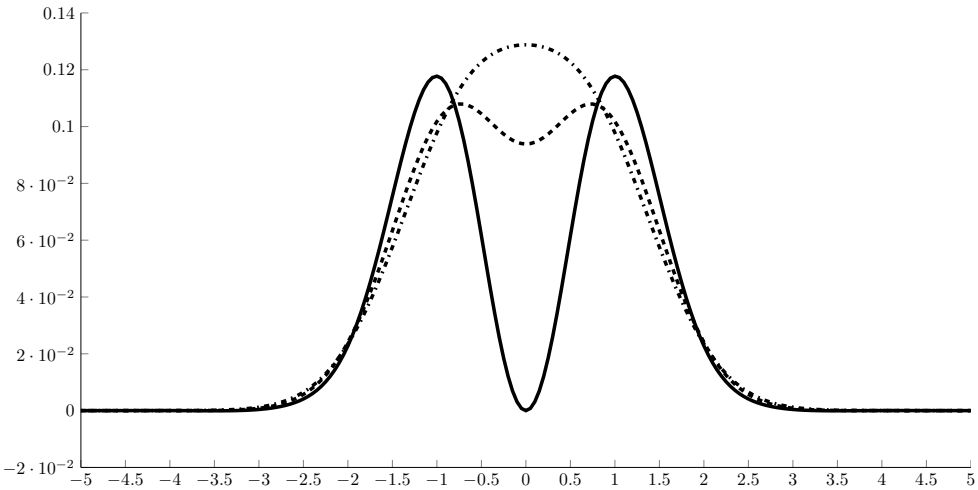

(a)

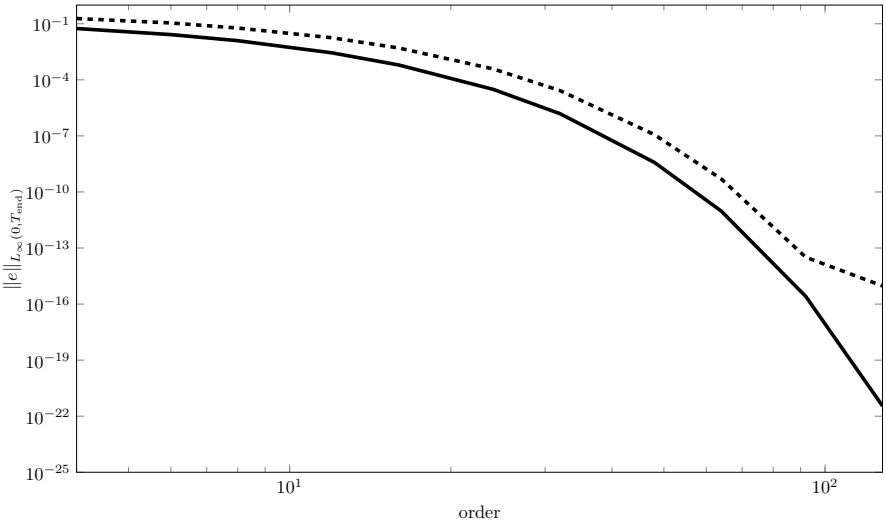

(b)

Fig. 4: Results for the BKW solution, example 1. (a) Snapshots of the distribution function for example 1, obtained with an order 16 simulation. The solid line is the initial distribution, the dashed line shows the solution at $t = 2$, the dashed dotted line is at $t = 4$. Note that the solution is radially symmetric at any time t. (b) Error plot for example 1. The dashed line is the $L_\infty-$error of $e := \|f_N - f\|_{L_2(\mathbb{R}^2)}$. The full line is the function $e^{-3/8N}$. The error reaches floating point precision.

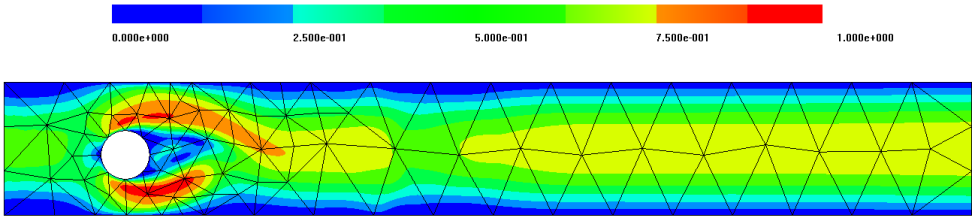

(a) Modulus of macroscopic velocity $|V(x)|$ at time $t = 1.1$.

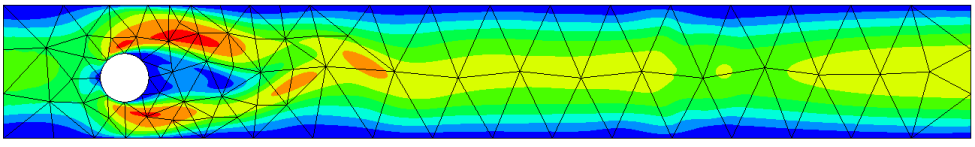

(b) Modulus of macroscopic velocity $|V(x)|$ at time $t = 2.0$.

Fig. 5: Results for example 2. Solution at different times t.

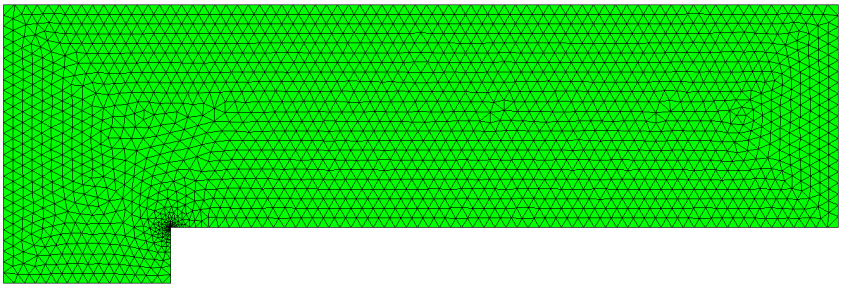

(a) Geometry and computational mesh for example 3.

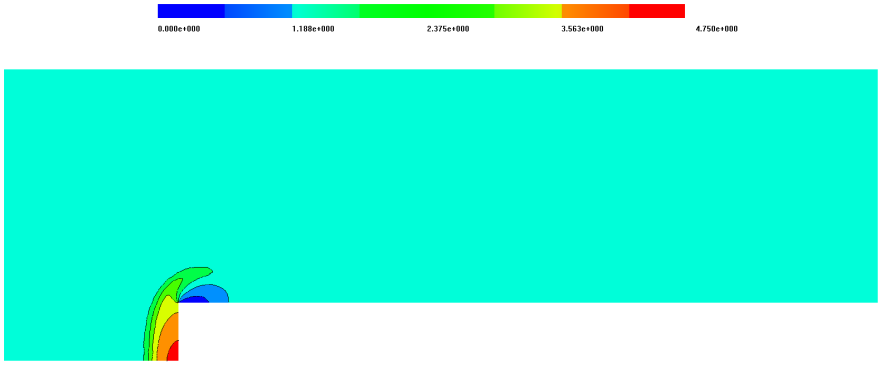

(b) Macroscopic Density $\rho(x)$ at time $t = 0.075$.

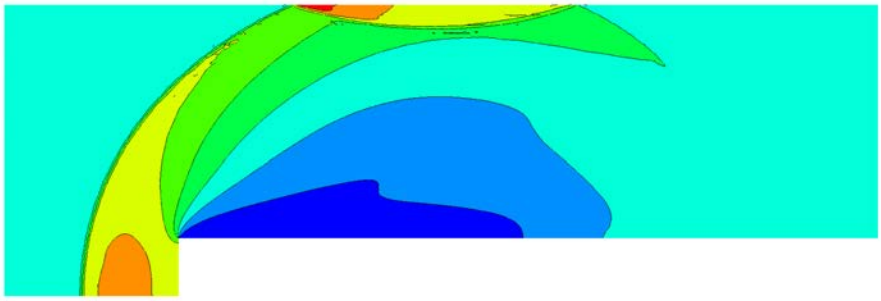

(c) Macroscopic Density $\rho(x)$ at time $t = 0.5$.

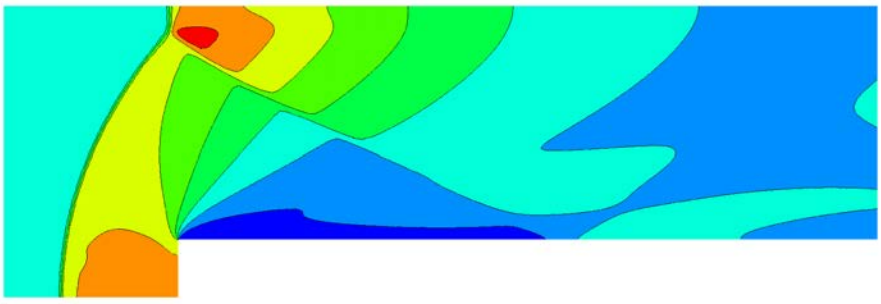

(d) Macroscopic Density $\rho(x)$ at time $t = 1.0$.

Fig. 6: Results for example 3.

REFERENCES

[1] G. A. Bird. *Molecular gas dynamics and the direct simulation of gas flows*, volume 42 of *Oxford Engineering Science Series*. The Clarendon Press, Oxford University Press, New York, 1995. Corrected reprint of the 1994 original, With 1 IBM-PC floppy disk (3.5 inch; DD), Oxford Science Publications.

[2] K. Nanbu. Direct simulation scheme derived from the boltzmann equation. I. monocomponent gases. *Journal of the Physical Society of Japan*, 49(5):2042–2049, 1980.

[3] H. Babovsky. On a simulation scheme for the Boltzmann equation. *Math. Methods Appl. Sci.*, 8(2):223–233, 1986.

[4] A. V. Bobylev. The method of the Fourier transform in the theory of the Boltzmann equation for Maxwell molecules. *Dokl. Akad. Nauk SSSR*, 225(6):1041–1044, 1975.

[5] A. Bobylev and S. Rjasanow. Difference scheme for the Boltzmann equation based on the fast Fourier transform. *European J. Mech. B Fluids*, 16(2):293–306, 1997.

[6] A. V. Bobylev and S. Rjasanow. Fast deterministic method of solving the Boltzmann equation for hard spheres. *Eur. J. Mech. B Fluids*, 18(5):869–887, 1999.

[7] L. Pareschi and B. Perthame. A fourier spectral method for homogeneous boltzmann equations. *Transport Theory and Statistical Physics*, 25(3-5):369–382, 1996.

[8] Lorenzo Pareschi and Giovanni Russo. Numerical solution of the Boltzmann equation. I. Spectrally accurate approximation of the collision operator. *SIAM J. Numer. Anal.*, 37(4):1217–1245, 2000.

[9] E. Fonn, P. Grohs, and R. Hiptmair. Polar spectral scheme for the spatially homogeneous boltzmann equation. Technical Report 2014-13, Seminar for Applied Mathematics, ETH Zürich, Switzerland, 2014.

[10] A. Ya. Ender and I. A. Ender. Polynomial expansions for the isotropic Boltzmann equation and invariance of the collision integral with respect to the choice of basis functions. *Phys. Fluids*, 11(9):2720–2730, 1999.

[11] B. A. De Dios, J. A. Carillo, and C.-W. Shu. Discontinuous galerkin methods for the multidimensional vlasovpoisson problem. *Mathematical Models and Methods in Applied Sciences*, 22(12):1250042, 2012.

[12] R. E. Heath, I. M. Gamba, P. J. Morrison, and C. Michler. A discontinuous Galerkin method for the Vlasov-Poisson system. *J. Comput. Phys.*, 231(4):1140–1174, 2012.

[13] C. Cercignani. *Mathematical methods in kinetic theory*. Plenum Press, New York, second edition, 1990.

[14] C. Cercignani, R. Illner, and M. Pulvirenti. *The mathematical theory of dilute gases*, volume 106 of *Applied Mathematical Sciences*. Springer-Verlag, New York, 1994.

[15] S. Rjasanow and W. Wagner. *Stochastic numerics for the Boltzmann equation*, volume 37 of *Springer Series in Computational Mathematics*. Springer-Verlag, Berlin, 2005.

[16] G. Kitzler and J. Schöberl. Efficient spectral methods for the spatially homogeneous boltzmann equation. Technical Report 13, Institute for Analysis and Scientific Computing, Vienna UT, 2013.

[17] M. Abramowitz and I. A. Stegun. *Handbook of mathematical functions with formulas, graphs, and mathematical tables*, volume 55 of *National Bureau of Standards Applied Mathematics Series*. For sale by the Superintendent of Documents, U.S. Government Printing Office, Washington, D.C., 1964.

[18] R. S. Krupp. *A Nonequilibrium Solution of the Fourier Transformed Boltzmann Equation*. PhD thesis, MIT, 1967.

[19] M. H. Ernst. Exact solutions of the nonlinear boltzmann equation. *Journal of Statistical Physics*, 34(5-6):1001–1017, 1984.